# Battery Cell Temperature Estimation Model and Cost Analysis of a Grid-Connected PV-BESS Plant

Md Mehedi Hasan*, S. Ali Pourmousav† and Tapan K. Saha‡
School of Information Technology and Electrical Engineering, The University of Queensland, Australia
Email: *mdmehedi.hasan@uq.edu.au, †a.pour@uq.edu.au, ‡saha@itee.uq.edu.au

***Abstract*—Battery cell temperature is an important factor in battery capacity degradation, performance, and safety. Elevated battery cell temperature, due to intense battery operation with high charging-discharging current and ambient temperature, accelerates battery capacity degradation as well as causing extra cooling cost. Therefore, it is indispensable to estimate battery cell temperature accurately for optimal BESS operation considering capacity degradation and its associated costs. The main objectives of this paper are to propose a linear model to estimate battery cell temperature using Autoregressive Integrated Moving Average with eXogenous variables (ARIMAX) considering strongly correlated independent variables and propose a cost function of PV plant with and without battery operation. The simulation results using field data show high accuracy of the proposed temperature estimation model without considering the complex thermal dynamics of the entire system. In addition, comprehensive cost functions are developed to show the benefit of integrating battery storage into a PV plant and determine influential factors to consider in any optimal battery operation systems.**

***Index Terms*—Battery cell temperature, degradation, ARIMAX, cost analysis, PV plant, BESS**

## I. Introduction

With the growth of large-scale photovoltaic (PV) and wind plants all over the world, the battery energy storage system (BESS) has become popular. BESS is essential for storing excess renewable generation when it is available and utilising it efficiently and economically during peak hours. It also plays a vital role in compensating the variability of renewable generation [1]. While technological improvement and cost reduction of electrochemical storage devices are taking place, battery degradation remains a big concern for the wide application of BESS [2]. To that end, an effective energy management system (EMS) is needed to operate battery in an optimal way by considering degradation and its associated costs. This can reduce unnecessary battery operation, which is responsible for higher degradation. To design a reliable EMS, it is important to derive a cost function for BESS operation considering all associated costs such as degradation and cooling costs. It helps to extend battery lifetime, which will economically benefit the entire system operation.

Battery capacity degrades due to charging-discharging operations as well as during idle condition [3], [4]. Among various responsible factors for battery capacity degradation, battery cell temperature has a crucial impact on accelerating battery capacity reduction [5]. In [6], it is shown that every 10°C battery cell temperature rise doubles the battery degradation. Accumulated heat generated by large-scale BESS placed in a confined container increases room temperature, which accelerates cooling system operation to keep the room temperature at an acceptable range. As a result, the elevated battery temperature increases operational cost for renewable plants with BESS. This way, it is essential to estimate battery temperature evolution with respect to battery operation and ambient temperature to have a better understanding of the incurred cost.

While a significant number of research studies has been conducted on thermal management of battery in electric vehicles (EVs) and plug-in hybrid electric vehicles (PHEVs) by proposing general models of battery thermal behaviour [7], [8], no such research has been conducted using linear modelling approach to estimate thermal behaviour of utility-scale BESS in connection with a grid-integrated renewable power plant. Detailed thermodynamic modelling to determine thermal behaviour of a single battery module is not feasible for large-scale BESS, where complex thermal interactions between thousands of battery cells are involved. This type of thermal modelling with intensive measurements and computational efforts, as suggested in [9], is not practicable for the EMS in utility-scale BESS because of the cost and scalability issues. Moreover, to the best of our knowledge, a comprehensive cost function for utility-scale BESS, including influential factors such as battery capacity degradation, cooling system operation and battery operational costs related to BESS operation, has not been reported in the literature.

In this paper, a data-driven battery cell temperature estimation model is proposed for a 600kW/760kWh BESS in a 3.275 MWp PV plant, located at the University of Queensland (UQ) Gatton campus, using a widely accepted linear statistical forecasting method, ARIMAX [10], [11], [12], which can be conveniently integrated with EMSs. A data-driven method does not require the physical dynamics of the BESS and thermal interactions between effective parameters. Instead, only historical data is needed to estimate future battery cell temperature. In addition, the proposed cost function in this study estimates total plant cost/benefit by considering battery capacity degradation, cooling cost, imported/exported energy from/to the grid, exported PV energy to the grid based in Feed-in-Tariff (FiT), and demand charge. A linear degradation model is adapted to calculate battery ageing. A comparison study has also been presented in this study to evaluate the total

cost of plant operation with and without BESS in a grid-tied PV plant. Actual field data from the UQ PV-BESS plant is used for modelling and evaluating the proposed methodologies. Extensive simulation results show the high accuracy of the proposed temperature model and prove the necessity of such models for optimal BESS operation.

The rest of the paper is organised as follows: Section II presents ARIMAX modelling for battery cell temperature estimation. Section III explains the cost formulations of PV plant with and without BESS. Section IV presents simulation study based on field data. Finally, the paper is concluded in Section V and future work is outlined.

## II. Battery Cell Temperature Modelling

In this study, ARIMAX is used to estimate battery cell temperature as a linear model. It is a powerful tool to outline the dynamics of a time series. The ARIMAX concept is proposed over ARIMA as a multivariate method that can include independent variables, which are important in the battery cell temperature model. In ARIMA, only dependent variable is regressed on its own lagged values (i.e., AR terms), error values generated in previous time steps by the model (i.e., MA terms) and the number of nonseasonal differences needed for stationarity of time-series data. In addition to ARIMA, ARIMAX model takes the impact of exogenous variables into account. In this study, the charging-discharging current of the battery and ambient temperature are considered as the external variables to estimate dependent variable, i.e., battery cell temperature, more accurately [3]. ARIMAX model can be mathematically represented as,

$$\hat{y}_\mathrm{t} = \beta x_\mathrm{t} + \phi_1 y_{\mathrm{t\text{-}1}} + ... + \phi_\mathrm{p} y_{\mathrm{t\text{-}p}} - \theta_1 z_{\mathrm{t\text{-}1}} - \cdots - \theta_\mathrm{q} z_{\mathrm{t\text{-}q}} + z_\mathrm{t} \quad (1)$$

where $\hat{y}_\mathrm{t}$ represents dependent variable based on differencing of time series data; $y_t$ is the dependent variable denoting actual time series; $x_\mathrm{t}$ represents exogenous inputs at time $t$ and $\beta$ is the coefficient of exogenous inputs; $z_t$ represents the forecast errors; and $\phi_\mathrm{p}$ and $\theta_\mathrm{q}$ are the estimated coefficients of the respective variables. $t$ denotes the time-step of the series.

The proposed model is classified as ARIMAX(p,d,q) model. There are three main parameters, namely $p$, $d$ and $q$, to be set to determine the model. $p$ is the number of auto-regressive terms, $d$ is the number of nonseasonal differences needed for converting the non-stationary time-series to a stationary one, and $q$ denotes the number of lagged forecast errors.

The identification of the model is performed in three steps. **First step** is to analyse the trend of time series to determine whether transformation is needed. In order to check the stationarity of the time series, statistical analysis will be carried out. Two tests are used in this study to check the stationarity of the time series:

- Augmented dickey fuller (ADF) unit root testing is chosen to examines the null hypothesis of a unit root [13].
- KwiatkowskiPhillips-Schmidt-Shin (KPSS) test is utilized to determine the stationarity of a time series around a mean or a linear trend [14].

Both tests collectively indicate the stationarity of a time series when existence of a unit root is rejected by ADF test and the mean/trend-stationarity of the time series is not rejected by KPSS test.

**Second step** is to find the best order of the auto-regressive model for estimating the battery cell temperature. An auto-regressive model predicts the dependent variable (i.e., battery cell temperature), where specific lagged values of the dependent variables are used as predictor variables. Partial autocorrelation function (PACF) is used to identify the order of the autorcorrelation or AR(p) model [15]. The other component of ARIMAX is the moving average (MA) with the order of $q$. In a time series model, a moving average term is a past error multiplied by a coefficient. Autocorrelation function (ACF) is used to determine the order (q) of MA model [15]. These methods will be used in Section IV for modelling using actual data.

**Third step** is to build the model using training dataset after identifying the $p$, $d$ and $q$ order. The coefficients of the model are identified during the training process. The trained model is then tested with a completely separate set of independent data (called test data), which has not being used during the training process, to evaluate the performance of the model. In order to quantify the accuracy of the battery cell temperature prediction, Root Mean Squared Error (RMSE), given in (2), is used as a standard measure.

$$\mathrm{RMSE} = \sqrt{\frac{\sum_{i=1}^{N} (T_{a_i} - T_{m_i})^2}{N}} \quad (2)$$

where $T_{a_i}$, $T_{m_i}$ and $N$ represent time series of actual battery cell temperature, predicted battery cell temperature using ARIMAX model, and the total number of samples, respectively.

## III. Cost Function Development

A comprehensive cost assessment considering the most effective parameters is able to render an opportunity to develop a cost function for the entire plant. Dominant factors such as battery degradation cost due to cycling and calendar ageing, cost of the cooling system, and the cost associated with charging-discharging operations of BESS have taken into account to develop a complete cost function for the plant. Appropriate formulation is derived for plant operation cost with and without BESS for comparison purposes, which helps to identify the effectiveness of the BESS integration in the plant. Such a comparison using simulation results will show the necessity of optimally operating battery to avoid the unnecessary cost. In this study, we run our study on a PV plant. However, the same methodology can be used for other renewable-based plants.

### A. PV plant cost with and without BESS

In this section, the plant operation costs with and without the BESS will be formulated step-by-step. The cost functions are developed based on the UQ Gatton plant in Australia, which has a local grid-connected BESS of Li-Polymer batteries [16]. The primary objectives of the plant are to fulfil campus electricity requirements and reduce demand charge.

*1)Total cost function with BESS:* Although BESS is primarily integrated into the PV plant to store excess PV energy and utilise the energy when grid price is high, its continuous operation in the plant causes extra cost. The dominant cost factors for operating a BESS are the cost associated with battery degradation, cooling system operation, and importing power from the grid to charge the BESS.

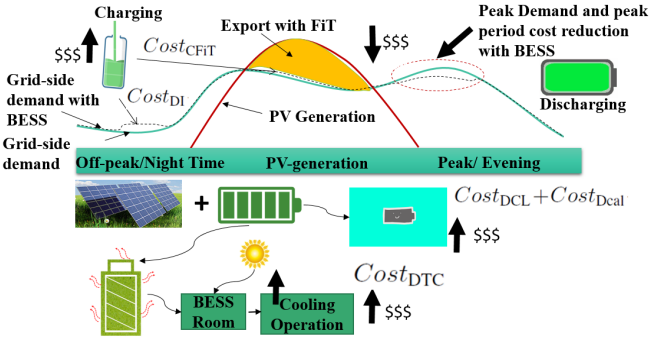


Fig. 1: Cost-benefit of the entire PV-BESS plant

Fig. 1 shows the daily cost-benefit associated with BESS operation in the plant. Continuous battery operation in charging and discharging modes as well as idle situation are responsible for battery degradation. Moreover, elevated temperature created by battery cell and ambient temperature in the confined BESS room accelerates the cooling system operation to maintain the room temperature within an acceptable range. Although a significant benefit is experienced by discharging operation of the BESS during peak hours, battery charging by the grid and avoiding selling excess PV generation to the grid at FiT price (yellow area in Fig. 1) will add to the overall cost of the system. As per operational rules, the BESS charging from the grid only takes place during the off-peak time, when the price is relatively lower. In addition, BESS will be charged by the excess PV power, if available. Therefore, this is considered as a cost in PV plant operation with BESS. The total PV plant cost, i.e., $Cost_{\text{WB}}$, on a daily basis is calculated using Eq. (3), where the cost associated with dominant factors are considered.

$$Cost_{\text{WB}} = Cost_{\text{DailyDeg}} + Cost_{\text{DTC}} + Cost_{\text{DI}} + Cost_{\text{CFiT}} \quad (3)$$

where $Cost_{\text{DailyDeg}}$ refers to the total cost associated with degradation; $Cost_{\text{DTC}}$ and $Cost_{\text{DI}}$ represent the cost of cooling system operation and imported grid-energy to charge the BESS, respectively. $Cost_{\text{CFiT}}$ is the cost of charging the BESS with excess PV energy in terms of opportunity loss to export energy to the grid at FiT rate.

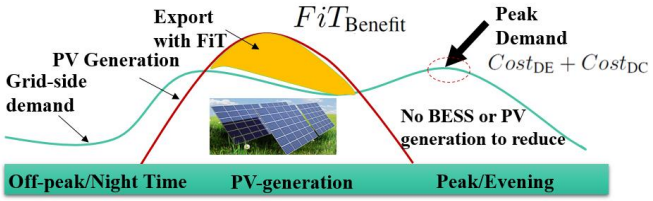


Fig. 2: Cost-benefit of the PV plant without BESS

*2)Total Cost of PV Plant Without BESS:* PV plant without BESS is only able to export energy to the grid at FiT. Due to unavailability of PV generation or storage during evening peak, the plant is unable to reduce the peak demand. Consequently, the demand charge cost[1] (shown in Fig. 2). Therefore, extra cost occurs for the PV plant without BESS. The total daily cost for PV plant without BESS, i.e., $Cost_{\text{WOB}}$, is estimated using Eq. (4).

$$Cost_{\text{WOB}} = Cost_{\text{DE}} + Cost_{\text{DC}} - FiT_{\text{Benefit}} \quad (4)$$

where $Cost_{\text{DE}}$ and $Cost_{\text{DC}}$ are the cost of energy and demand charge during peak hours, respectively. $FiT_{\text{Benefit}}$ refers to the benefit from exporting PV energy to the grid.

### *B. Battery Degradation Cost*

Degradation of a battery is a continuous process, where several factors affect degradation at the same time. A battery undergoes charge and discharge as well as idle situation throughout its lifetime. Therefore, both processes (i.e., cycling and calendar ageing processes) continuously drive battery ageing. A simplified linear cyclic and calendar ageing models are formulated in this study to quantify the degradation of the BESS. Accordingly, a cost function is developed to quantify the cost of degradation on a daily basis. The hourly degradation cost is calculated using Eq. (5).

$$Cost_{\text{DEG}} = Cost_{\text{BESS}} \times (DEG_{\text{Cyclic}} + DEG_{\text{Calendar}}) \quad (5)$$

where $Cost_{\text{DEG}}$ presents the total degradation cost; $DEG_{\text{Cyclic}}$ and $DEG_{\text{Calendar}}$ represent the degradation of BESS because of cyclic and calendar ageing mechanisms, respectively. The total cost of BESS is calculated considering energy and power costs, i.e., $Cost_{BESS} = C_{\text{kWh}}(\$) \times E_{\text{cap}}(kWh) + C_{\text{kW}}(\$) \times P_{\text{cap}}(kW)$. Here, the BESS rated power and energy capacity is represented by $E_{\text{cap}(kWh)}$ and $P_{\text{cap}}(kW)$, respectively and prices per $kWh$ and $kW$ are denoted by $C_{\text{kWh}}$ and $C_{\text{kW}}$.

*1)Cyclic Ageing:* Degradation of a battery for cyclic ageing mechanism during a specific time is quantified with respect to the energy throughput for that time interval, and the entire energy throughput of the BESS throughout its lifetime, given in $DEG_{Cyclic} = E_{\text{Th}}/B_{\text{LT}}$. Here, $E_{\text{Th}}$ and $B_{\text{LT}}$ are representing the total energy throughput for a given time interval and the total BESS energy throughput until it reaches its end of life (EoL), respectively. Charging and discharging activities of BESS are observed using Eq. (6) for each time-interval to quantify the energy throughput.

$$E_{\text{Th}} = \eta_{\text{CH}} \sum_{j=1}^{t} P_{j,\text{CH}} \times h + \eta_{\text{DCH}} \sum_{j=1}^{t} \mid P_{j,\text{DCH}} \mid \times h \quad (6)$$

where $E_{\text{Th}}$ is the total energy throughput; $\eta_{\text{CH}}$ and $\eta_{\text{DCH}}$ represent the efficiency of charging and discharging operations, respectively; and $P_{j,\text{CH}}$ and $P_{j,\text{DCH}}$ are the real power in kW for charging and discharging operations, respectively. Total energy throughput of the BESS is calculated using Eq. (7), which considers the battery's EoL, total rated cycle number

[1]It is the cost of a single monthly peak demand that should be paid alongside energy cost. It is calculated by averaging the measured instantaneous power in pre-defined intervals.

at the rated depth of discharge (DoD), and the rated energy capacity of the BESS.

$$B_{\text{LT}} = 2 \times DoD_{\text{R}} \times \frac{\eta_{\text{CH}}}{\eta_{\text{DCH}}} \times E_{\text{cap}} \times \sum_{j=0}^{N_{\text{R}}} (1 + \frac{EoL - 1}{N_{\text{R}}} \times j) \quad (7)$$

where $B_{\text{LT}}$ is the total $kWh$ throughput energy of the battery over its lifetime. $DoD_{\text{R}}$ represents the rated DoD for the BESS; $E_{\text{cap}}$ is the actual energy capacity of the BESS at the beginning of its operation in the field; and $N_{\text{R}}$ is the rated battery cycles.

*2) Calendar Ageing:* Calendar ageing is estimated by counting the number of idle hours experienced by the BESS and the total calendar life of the battery, as given in $DEG_{\text{Calendar}} = \mathbb{T}_{\text{Idle}}/\mathbb{T}_{\text{Life}}$. Here, $\mathbb{T}_{\text{Idle}}$ and $\mathbb{T}_{\text{Life}}$ are the time in which battery is idle within a specific period of time and the entire calendar life of the BESS, respectively. Hourly idle time during a day is calculated using, $\mathbb{T}_{\text{Idle}} = \sum_{j=1}^{t} S_{\text{j}} \times h$. Here, $S_{\text{j}}$ is the ON/OFF status of the battery; $\mathbb{T}_{\text{Idle}}$ represents the accumulated idle time of the battery until time $t$. The status of the battery is counted and accumulated for a certain period of time as per requirement. The battery is considered OFF when $P_{\text{j,CH}} = 0$ and $P_{\text{j,DCH}} = 0$ at a given time. Otherwise, battery is under operation, i.e., ON.

The total battery calendar life is calculated using $\mathbb{T}_{\text{Life}} = 365 \times 24 \times \mathbb{T}_{\text{RATED}}$, where $\mathbb{T}_{\text{RATED}}$ is the rated calendar life of the battery in year. Hourly quantified degradation achieved from the aforementioned equations is calculated on a daily basis by observing degradation for 24 hours. The total degradation cost on daily basis can be calculated as: $Cost_{\text{DailyDeg}}(t) = \sum_{j=1}^{24} Cost_{\text{DEG},j}$.

### C. Cooling Cost

The active cooling system at the UQ Gatton plant consists of rack fans and air-conditioning unit with 7.7kW cooling capacity, which is dedicated to keeping the confined storage room temperature at an acceptable range. 85% of power is consumed by compressor unit rated at 2.3kW, compared to the condenser-evaporator fans rated at 0.43kW. The power consumption by rack fans is 0.36kW.

Operation of each cooling unit is controlled by certain rules, given in Eq. (8), which shows the type of operation in different thermal conditions. Minute-by-minute temperature values are considered to calculate the total energy consumption and associated cost by the cooling systems.

$$C_{\text{Cool}}(T) = \begin{cases} C_F, & T_R < 23°C \\ C_{COM} + C_F, & T_R \geq 23°C \\ C_{COM} + C_F + C_{RF}, & (T_C \geq 29°C) \wedge (T_R \geq 23°C) \\ C_F + C_{RF}, & (T_C \geq 29°C) \wedge (T_R < 23°C) \end{cases} \quad (8)$$

where $C_{\text{Cool}}$ represents the hourly cooling cost; $T_R$ and $T_C$ refer to the battery room temperature and average battery cell temperature, respectively. $C_{\text{COM}}$, $C_{\text{F}}$ and $C_{\text{RF}}$ are the cost function of each cooling systems' component, namely compressor, fan of air-conditioning unit, and rack fans on top of each battery bank, respectively. Daily cooling cost is calculated using $Cost_{\text{DTC}} = \sum_{n=1}^{t=24} C_{\text{Cool}}(n)$, where $Cost_{\text{DTC}}$ refers to the total daily energy cost of cooling system operation. Due to different energy tariff during a day, shown in (9), hourly cost is calculated using hourly energy consumption, by different cooling system units.

$$\tau(t) = \begin{cases} 6.545¢/kWh, & t \in [11PM, 12AM), (12AM, 7AM] \\ 11.78¢/kWh, & t \in [7AM, 11PM] \end{cases} \quad (9)$$

where $\tau(t)$ represents the local time-of-use (TOU) tariff throughout a day.

### D. Demand Charge

The demand charge is calculated based on the maximum apparent power (kVA). kVA is calculated for each 30 minutes period using, $\text{kVA} = \sqrt{(\text{kW})^2 + (\text{kVAr})^2}$. The maximum kVA demand is estimated for each billing period (30 days). Therefore, the recorded peak value is used for the entire month's demand charge calculation, $Cost_{\text{MDC}} = \text{kVA}_{\text{Maximum}} \times (\sigma_{\text{DUoS}} + \sigma_{\text{TUoS}})$, where $Cost_{\text{MDC}}$ represents the demand charge for monthly billing period; $\sigma_{\text{DUoS}}$ and $\sigma_{\text{TUoS}}$ denote distribution use of system (DUoS) and transmission use of system (TUoS) charges ($\sigma_{\text{DUoS}} = \$12.49/kVA/month$ and $\sigma_{\text{TUoS}} = \$1.169/kVA/month$) per month, respectively.

As demand charge is calculated based on 30-day period, daily demand charge cost, i.e., $Cost_{\text{DC}}$, is calculated by multiplying the cost of demand charge per kVA per month by the peak monthly power demand.

### E. Cost of imported energy from the grid and demand charge

$Cost_{\text{DI}} = \sum_{n=1}^{5} E_{\text{C}}(t) \times \tau(t)$ is utilised to calculate the daily cost associated with the grid imported energy for charging the BESS. Here, $Cost_{\text{DI}}$ is the total daily cost of imported energy from the grid. Hourly imported grid energy is represented by $E_{\text{C}}$. The BESS is charged by the grid between $1^{st}$ and $5^{th}$ hours of each day.

The BESS is playing a vital role by reducing peak load during discharging. In the absence of the BESS, PV plant will need to buy the energy from the grid with the peak-period tariff. The cost associated with the energy is calculated using $Cost_{\text{DE}} = \sum_{n=18}^{23} E_{\text{D}}(t) \times \tau(t)$, where $Cost_{\text{DE}}$ represents the total daily cost of energy that is purchased from the grid during peak demand. The BESS is discharged between $18^{th}$ and $23^{th}$ hours of each day for peak shaving, when the grid energy cost is more and peak demand is more prone to happen. The hourly energy by discharging the BESS is represented by $E_{\text{D}}$.

### F. FiT Benefit

The benefit obtained by the FiT scheme is calculated based on the PV generated energy that is exported to the grid. The cost of charging the BESS with PV energy, $Cost_{\text{CFit}}$ is calculated using $Cost_{\text{CFiT}}(t) = P_{\text{CPV}}(t) \times h \times \xi_{\text{FiT}}$ and $FiT_{\text{Benefit}}(t) = P_{\text{EPV}}(t) \times h \times \xi_{\text{FiT}}$ is used to find out the cost of the exported PV energy. Here, $P_{\text{CPV}}$ and $P_{\text{EPV}}$ are the PV generated power for charging and exporting to the grid, respectively; and $\xi_{\text{FiT}} = 2.356¢/kWh$ refers to FiT rate.

## IV. Simulation Study

In this study, a significant number of data, that covers numerous plausible combinations of charging-discharging and

ambient temperature operations, is used to establish the battery cell temperature model and cost analysis for the PV plant.

○ Data Selection for ARIMAX Model:

- To train the ARIMAX model, 12 months equivalent data with 1-minute sampling rate from 1st April 2016 to 31st March 2017 have been selected, which consists of 516,960 samples (359 days).
- To evaluate the ARIMAX model, a separate 30 days of test data is used from 1st April 2017 to 31st October 2017.

○ Data Selection for Cost Analysis:

- 13 months data, sampled every 1 minute, from 1st April 2016 to 30th September 2017 have been selected for this purpose. Also, 13 days of data with seasonal differences are selected to assess seasonality impact on the PV plant.
- 1 day with the highest peak demand from each billing period is selected for demand charge calculation for the entire billing period.

### *A. ARIMAX Estimation Model Outcomes*

As mentioned in section II, PACF, ADF-KPSS and ACF tests are used to find the best order of $p$, $d$ and $q$, respectively, prior to modelling.

Stationarity of the time series is checked using ADF and KPSS tests. The p-value was about zero, which is far below 0.05 (for 95% confidence interval). It gives the indication of rejecting the null hypothesis, that is not having a unit root in the time series. In addition, KPSS test fails to reject the null hypothesis with a p-value less than 0.01 and test critical values of 0.347, 0.462 and 0.744 for 10%, 5% and 1% confidence intervals, respectively. The test critical values are more than the test statistic value, 0.0733. Therefore, it can be concluded that the time series data is stationary; hence, differencing the time series data is not required. Therefore, the order of I(d) will be 0 or $I(0)$.

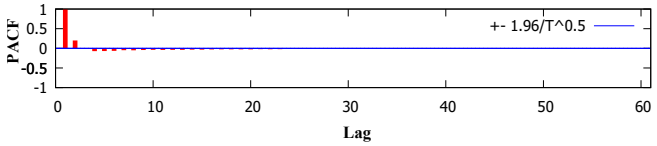


Fig. 3: PACF plot for the training data set

Fig. 3 shows the PACF values for different lags of data. An approximate test that a given partial correlation is zero (at a 95% significance level) is given by comparing the sample partial autocorrelations against the critical region with upper and lower limits given by $\pm 1.96/\sqrt{T}$, where $T$ is the number of samples of the time series. There is a cut-off experienced after the lag 26, which suggests an AR model with order of 26, i.e. $AR(26)$.

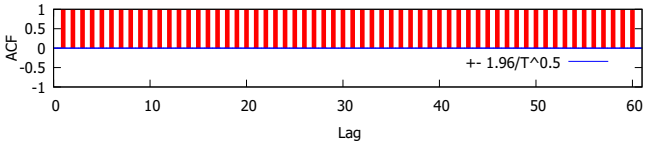


Fig. 4: ACF plot for the training data set

Fig. 4 shows the autocorrelation values of different lags. It shows that there is no cut-off, where the peak of the autocorrelation value for lag falls below the critical region. The value remains almost the same even after 60 lags. It, therefore, indicates the order of the MA model at 0 or $MA(0)$.

From the above analysis with trained data, the order of model is found to be ARIMAX(26,0,0). This means that the best model has 26st order of autoregressive model with 0 order moving average and non-seasonality time-series data.

Training data is used for modelling, and the hourly-averaged RMSE histogram of the 30 days of estimation using test data is shown in Fig. 5. It shows that the majority of the hourly estimation (63.61%) yields equal or below 1°C of RMSE. Only 14.86% of hourly estimation renders RMSE beyond 2°C. It can be observed from the figure that 129 hours of estimation yield only 0.21°C to 0.4°C RMSE. Most of the hourly estimation errors are within 0.01°C and 1.19°C RMSE range, which suggests an accurate estimation of the battery cell temperature.

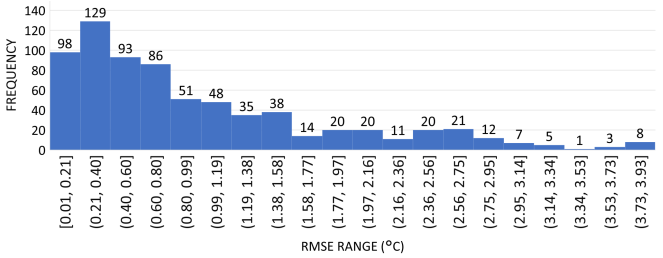


Fig. 5: Histogram of hourly RMSE of battery cell temperature for 30 test days using ARIMAX model

### *B. Cost Analysis*

Fig. 6 to Fig. 8 show the total operational cost of the plant and comparison between PV plant with and without BESS for 13 selected days of the equivalent number of month.

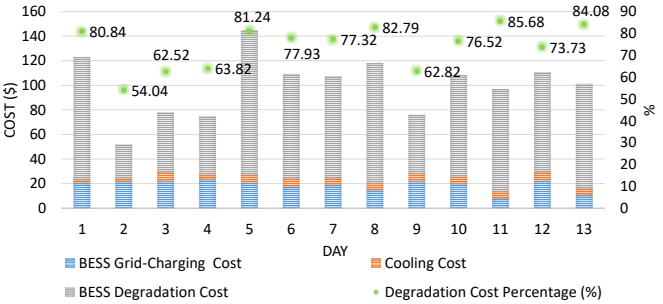


Fig. 6: Daily cost associated with BESS operation in the plant

Fig. 6 presents the daily cost of each dominant factor for operating the BESS. It is clear from the figure that the cooling cost has less impact on daily total cost compared to the battery degradation and charging cost from the grid. The cooling cost has 5.6% impact on the total cost on average, where the grid charging and degradation costs are responsible for 20.3% and 74.1% of the total daily cost on average, respectively. Also, the variation in the cooling cost is strongly correlated with the BESS cell temperature and seasonality. There are five days in which the degradation cost is more than 80% of the total daily cost associated with the BESS in the plant because of higher charge-discharge operations and temperature.

Fig. 7 shows the monthly demand charges in 13 months with and without BESS. 80% of the time, the demand charge for each billing period without BESS is around $30,000, where only 20% yields demand charge between $50,000 and $60,000. The number signifies the importance of demand charge management in each billing period. It is noticeable that the BESS is providing utmost efforts in reducing the charge during each billing period. 46.1% of the time, the demand charge is reduced by more than 10% with the help of BESS. Except for only 0.48% cost reduction in 4$^{th}$ month, the demand charge is reduced by more than 5% in more than 90% of the times with the help of BESS in the plant.

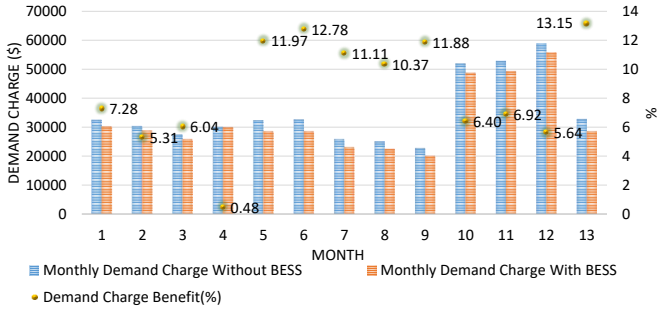


Fig. 7: Monthly demand charge with and without BESS

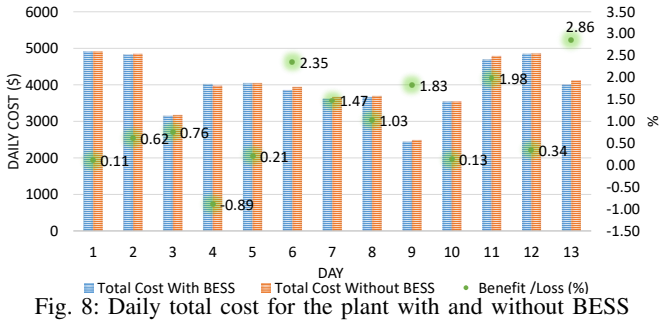


Fig. 8: Daily total cost for the plant with and without BESS

Total daily plant cost is compared in Fig. 8 with and without BESS for 13 different test days from 13 months. It can be seen that only three days yield more than $90 benefits with BESS and the rest of the days show a profit of less than $50. On day four, there is about 1% loss that encountered in the plant with BESS in comparison to the PV plant operation cost without BESS. However, more than 90% of times, there is some sort of benefit out of BESS (46.1% of times, more than 1% benefit with BESS is obtained).

As per the above analyses, it is clear that BESS plays a vital role by reducing the demand charge from the monthly bill. However, when it comes to the total cost between PV plant with and without BESS, the benefit with BESS is not significant most of the time. Most influential cost factor, namely battery degradation cost, is responsible for the reduction in the BESS benefit. Therefore, it is important to establish an operational algorithm for BESS to reduce battery degradation. In addition, operating BESS during peak demand with higher magnitude will increase the benefit.

## V. Conclusion

In this study, a battery cell temperature estimation model is proposed based on the ARIMAX method. A large historical data-set with 1-minute sampling rate is used to train the model and a completely different set of data is chosen for evaluating the developed model. Based on the simulation results, the estimated battery cell temperature was below 2°C most of the time, which is quite satisfactory for the EMS application. In addition to the estimation model, a cost-benefit analysis is carried out considering battery operational cost in the PV plant. Cost functions are developed to render a comparison study between PV plant with and without BESS. The cost-benefit analyses show an untimely battery capacity loss (as a result of drastic battery operation and excess battery cell temperature incurred extra cost), which reduces the benefit from BESS in the plant. It also proves that the BESS integration into the PV plant increases the overall net benefits, which can be further improved by alleviating temperature-dependent costs. In our future works, the ARIMAX estimation model will be utilised to develop an optimal battery operation algorithm in the EMS considering battery degradation cost and thermal effects.

## References


[1] S. Pourmousavi and T. K. Saha, "Evaluation of the battery operation in ramp-rate control mode within a pv plant: A case study," *Solar Energy*, vol. 166, pp. 242–254, 2018.

[2] B. Scrosati and J. Garche, "Lithium batteries: Status, prospects and future," *Journal of power sources*, vol. 195, no. 9, pp. 2419–2430, 2010.

[3] M. M. Hasan, S. A. Pourmousavi, F. Bai, and T. K. Saha, "The impact of temperature on battery degradation for large-scale bess in pv plant," in *Universities Power Engineering Conference (AUPEC), 2017 Australasian*. IEEE, 2017, pp. 1–6.

[4] F. Leng, C. M. Tan, and M. Pecht, "Effect of temperature on the aging rate of li ion battery operating above room temperature," *Scientific reports*, vol. 5, p. 12967, 2015.

[5] A. Millner, "Modeling lithium ion battery degradation in electric vehicles," in *Innovative Technologies for an Efficient and Reliable Electricity Supply (CITRES), 2010 IEEE Conference on*. IEEE, 2010, pp. 349–356.

[6] O. Gross and S. Clark, "Optimizing electric vehicle battery life through battery thermal management," *SAE International Journal of Engines*, vol. 4, no. 1, pp. 1928–1943, 2011.

[7] M. Doyle, J. Newman, A. S. Gozdz, C. N. Schmutz, and J.-M. Tarascon, "Comparison of modeling predictions with experimental data from plastic lithium ion cells," *Journal of the Electrochemical Society*, vol. 143, no. 6, pp. 1890–1903, 1996.

[8] T. M. Bandhauer, S. Garimella, and T. F. Fuller, "A critical review of thermal issues in lithium-ion batteries," *Journal of the Electrochemical Society*, vol. 158, no. 3, pp. R1–R25, 2011.

[9] W. Gu and C. Wang, "Thermal-electrochemical modeling of battery systems," *Journal of The Electrochemical Society*, vol. 147, no. 8, pp. 2910–2922, 2000.

[10] H.-T. Yang, C.-M. Huang, and C.-L. Huang, "Identification of armax model for short term load forecasting: An evolutionary programming approach," in *Power Industry Computer Application Conference, 1995. Conference Proceedings., 1995 IEEE*. IEEE, 1995, pp. 325–330.

[11] G. P. Zhang, "Time series forecasting using a hybrid arima and neural network model," *Neurocomputing*, vol. 50, pp. 159–175, 2003.

[12] J. H. Cochrane, "Time series for macroeconomics and finance," *Manuscript, University of Chicago*, 2005.

[13] W. A. Fuller, *Introduction to statistical time series*. John Wiley & Sons, 2009, vol. 428.

[14] N. Korolko, Z. Sahinoglu, and D. Nikovski, "Modeling and forecasting self-similar power load due to ev fast chargers," *IEEE Transactions on Smart Grid*, vol. 7, no. 3, pp. 1620–1629, 2016.

[15] G. E. Box, G. M. Jenkins, G. C. Reinsel, and G. M. Ljung, *Time series analysis: forecasting and control*. John Wiley & Sons, 2015.

[16] M. Alam, R. Yan, T. Saha, A. Chidurala, and D. Eghbal, "Learning from a 3.275 mw utility scale pv plant project," in *CIGRé*, 2016.